Catal Lett (2008) 126:100–105
DOI 10.1007/s10562-008-9587-1

$MgO–Al_2O_3$ Mixed Oxides-Supported Co–Mo-Based Catalysts for High-Temperature Water–Gas Shift Reaction

Huifang Wang · Yixin Lian · Qing Zhang · Qiaoling Li · Weiping Fang · Yiquan Yang

Received: 18 May 2008 / Accepted: 9 July 2008 / Published online: 13 August 2008

Abstract $MgO–Al_2O_3$ mixed oxides were prepared and used as the support of Co–Mo-based water–gas shift reaction (WGSR) catalysts. X-ray diffraction (XRD) characterization showed that the $MgO–Al_2O_3$ mixed oxides support is composed of MgO, γ-Al_2O_3, and magnesia–alumina spinel. The $MgO–Al_2O_3$ mixed oxides-supported Co–Mo-based catalysts exhibited high shift activity at high temperature (360–450 °C) and high stability. The addition of potassium enhanced the activities but affected adversely the stabilities of Co–Mo-based catalysts. ESR characterization shows that the Mo^{5+} species are not connected with the WGSR activity. Magnesium in the support may be closely related with the formation of formate species intermediate for the WGSR.

Keywords $MgO–Al_2O_3$ mixed oxides · Spinel · Water–gas shift · Co–Mo-based catalysts

1 Introduction

Water–gas shift reaction (WGSR, i.e., $CO + H_2O \leftrightarrow CO_2 + H_2$) is an important process used to produce hydrogen or adjust the CO/H_2 molar ratio in synthesis gas [1–3]. An emerging application for the WGSR is in the field of fuel cell for removing CO, which is a strong poison of proton exchange membrane (PEM) anode catalysts [4, 5]. In the industrial processes such as methanol synthesis and ammonia synthesis, where considerable quantities of H_2 are required, two types of catalysts are widely used, i.e., Fe–Cr catalysts used for the high-temperature shift (310–450 °C) and Cu–Zn catalysts used for the low-temperature shift (200–250 °C) [1, 3, 6, 7]. However, these two types of WGSR catalysts are high sensitive to sulfur contaminations. It is essential to reduce the content of the sulfur-containing compounds (or even remove them) in the feedstock prior to the shift process.

Recently, a new type of sulfur-tolerant WGSR catalysts, i.e., supported sulfided Mo-based catalysts, has been specifically designed for high sulfur-containing feedstock [1, 8–19]. Łaniecki et al. [13, 16, 18] investigated the Y-type zeolite, alumina, titania, zirconia, and $TiO_2–ZrO_2$ mixed oxides-supported molybdenum sulfide catalysts for the WGSR. It is well known that alkali and Groups VIII metal additives enhance the activities of the Mo-based WGSR catalysts [1, 9, 19]. Industrially, Al_2O_3-supported K–Mo catalysts promoted with cobalt or nickel are widely used as sulfur-tolerant WGSR catalysts, which also tolerate small amounts of O_2, HCN, and C_6H_6 in the feedstock [9, 17, 20]. However, it is worth noting that the mobility of alkali promoter in the industrial catalysts affects adversely the stability of the catalysts. At higher operation temperature, the potassium loss takes place more easily [21]. Therefore, developing a kind of potassium-free catalyst or stabilizing the potassium component in the potassium-containing catalysts is the way to solve this practical problem. For commercial high-temperature shift catalysts, $MgAl_2O_4$ spinel was used as the support of K-free Co–Mo-based catalysts [20, 22, 23]. Very recently, potassium-free catalysts such as molybdenum carbide catalysts [24, 25] and $Ni–MoO_2$ catalysts [26] were found to be highly active for the WGSR, however, the complicated preparation impede the industrial application of these catalysts.

Compared to the conventional support (Al_2O_3), mixed oxides such as $SiO_2–Al_2O_3$ and $MgO–Al_2O_3$ were proved

H. Wang · Y. Lian · Q. Zhang · Q. Li · W. Fang · Y. Yang (✉)
College of Chemistry and Chemical Engineering, Xiamen University, Xiamen 361005, People's Republic of China
e-mail: yyiquan@xmu.edu.cn

to be excellent supports of the hydrotreating catalysts [27]. In the present work, MgO–Al_2O_3 mixed oxides were prepared and used as the support of Co–Mo-based sulfur-tolerant water–gas shift catalysts. The catalyst stability as a function of the reaction time was investigated. X-ray diffraction (XRD) measurements were carried out to probe the structure of magnesium species in the support. Electron spin resonance (ESR) measurements were used to determine whether the Mo^{5+} species play roles in the catalytic mechanism.

2 Experimental

2.1 Support Preparation

The MgO–Al_2O_3 support was prepared by mechanical mixing method. Typically, calculated amounts of light magnesia and pseudo-boehmite were mixed with a blender to produce a uniform powder mixture, to which HNO_3 aqueous solution and methyl cellulose were added, blended, and then kneaded until the waterish paste was suitable for extrusion molding. Subsequently, the paste was extruded into cylinders with 4 mm in diameter and 5–6 mm in length. The obtained cylinders were then dried at 110 °C, and finally calcined at 700 °C for 3 h. The molar ratio of MgO to Al_2O_3 of the support was chosen to be 1:1. The BET surface area of the support thus prepared was measured to be 130 $m^2\ g^{-1}$. The obtained mixed oxides support was denoted as MgO–Al_2O_3. The $MgAl_2O_4$ spinel supports (S_{BET} = 160 $m^2\ g^{-1}$) were prepared according to the method reported in [28]: a solution of $NaAlO_2$ mixed rapidly with a solution of $Mg(NO_3)_2$, and the pH value was controlled to 9.2–9.4 by dropping Na_2CO_3 aqueous solution. The obtained precipitate was washed three times with hot water. Subsequently, the precipitate was dried at 100 °C and calcined at 600 °C for 3 h.

2.2 Catalyst Preparation

The catalysts were prepared by incipient wetness co-impregnation method. In a typical preparation of the Co–Mo–K/MgO–Al_2O_3 catalyst, the required quantities of $(NH_4)_6Mo_7O_{24} \cdot 4H_2O$, $Co(NO_3)_2 \cdot 6H_2O$, and K_2CO_3 were dissolved in deionized water, to which ammonia was added dropwise until the precipitate was fully dissolved under stirring. With the obtained aqueous solution MgO–Al_2O_3 support was impregnated for 8 h, followed by drying at 120 °C and calcining at 350 °C for 4 h. For a comparison, Co–Mo catalysts supported on γ-Al_2O_3 (commercial sample, S_{BET} = 200 $m^2\ g^{-1}$) and $MgAl_2O_4$ were prepared by the same method. The amounts of Mo and Co precursors were calculated in order to obtain 50% theoretical monolayer coverage. The theoretical monolayer coverage was calculated based on the surface densities of four Mo atoms per nm^2 support and 1.1 Co atoms per nm^2 support (approximately equals to Ni/nm^2 support) [17]. The catalysts thus prepared CoO–MoO_3–K_2O/γ-Al_2O_3 (1.5–8.5–*x*/100), CoO–MoO_3–K_2O/$MgAl_2O_4$ (1.2–7.1–*x*/100), and CoO–MoO_3–K_2O/MgO–Al_2O_3 (1.0–6.0–*x*/100) were denoted as Co–Mo–K_x/Al_2O_3, Co–Mo–K_x/$MgAl_2O_4$, Co–Mo–K_x/MgO–Al_2O_3, respectively.

2.3 Catalytic Activity Testing

Catalytic activity tests were carried out in a stainless-steel tubular microreactor. Before evaluation, the oxidic catalysts (0.5 mL) were presulfided in situ at 400 °C for 4 h with a H_2/CO/CS_2 flow, which was introduced by saturation of a H_2/CO mixtures (95/5, v/v) carrier flowing through CS_2 [29]. The feedstock of CO/H_2 (3/7, v/v) was mixed into a high pressure cylinder, to which 2–5% (vol. %) of N_2 was added as internal standard. Water was pumped with a precision injection pump into a steam generator. The obtained steam was introduced into the reactor along with the $CO/H_2/N_2$ flow. CO conversion was analyzed by using an on-line gas chromatograph equipped with a thermal conductivity detector (a 5 A molecular sieve column, 2.0 m × 8 mm) when the steady-state achieved.

2.4 Catalyst Characterization

X-ray diffraction patterns were measured with a PANalytical X'Pert PRO diffractometer with Cu $K\alpha$ radiation (λ = 0.154 nm). Phases present in the samples were identified by using X'Pert HighScore software.

ESR measurements were performed by using a Bruker EMX-10/12 EPR spectrometer at room temperature. All spectra were obtained with a microwave power of 54.1 mW, modulation amplitude of 6.00 G, modulation frequency of 100 KHz, and a time constant of 40.96 m s.

3 Results

3.1 XRD Characterization

Figure 1 shows the XRD patterns of the references and the support (γ-Al_2O_3, $MgAl_2O_4$, pseudo-boehmite, MgO, and support). The peaks at 2θ = 19.1, 31.3, 36.8, 43.0, 45.4, 60.2, 62.3, and 66.4° were detected on the MgO–Al_2O_3 support (Fig. 1d). These peaks comprise of several groups of peaks arising from different crystal phases. The peaks at 2θ = 43.0 and 62.3° for the support matched well to the characteristic peaks specific to MgO (PDF code: 01-079-0612). The peaks at 2θ = 19.1, 31.4, 37.0, 45.0, 59.6, and

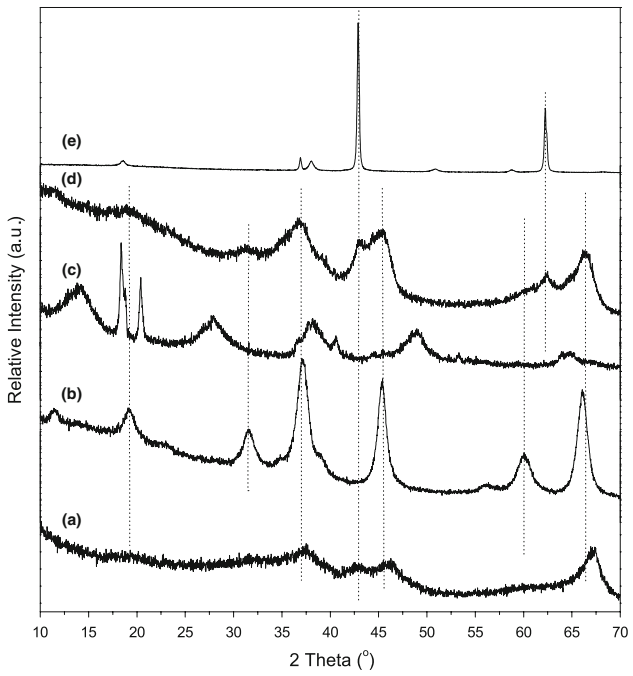

Fig. 1 XRD patterns of the references and the support: (**a**) γ-Al_2O_3, (**b**) $MgAl_2O_4$, (**c**) pseudo-boehmite, (**d**) MgO–Al_2O_3 support, and (**e**) MgO

65.6° appearing in $MgAl_2O_4$ spinel (PDF code: 01-073-1959) and the peaks at 2θ = 37.4, 42.8, 45.8, and 67.3° appearing in γ-Al_2O_3 (PDF code: 00-004-0880) occurred on the MgO–Al_2O_3 support as well. Obviously, the overlapped peaks on the support broadened. This suggests that the binary MgO–Al_2O_3 support is composed of mixed oxides of MgO, γ-Al_2O_3, and $MgAl_2O_4$ spinel. Theoretically, the formation of $MgAl_2O_4$ requires an equal molar ratio of MgO to Al_2O_3. In this study, the co-existence of γ-Al_2O_3 and $MgAl_2O_4$ shows that only a part of pseudo-boehmite and magnesia transforms to $MgAl_2O_4$.

3.2 Catalytic Activity

Figure 2 presents the CO conversions over the MgO–Al_2O_3, γ-Al_2O_3, and $MgAl_2O_4$-supported Co–Mo catalysts at various potassium loadings ranging from 0 to 6 wt.%. The potassium-free catalysts, Co–Mo/MgO–Al_2O_3, Co–Mo/Al_2O_3, and Co–Mo/$MgAl_2O_4$ catalysts, exhibited low activities for the WGRR at 220 °C. The Co–Mo/MgO–Al_2O_3 catalyst exhibited the highest activity (activity order, Co–Mo/MgO–Al_2O_3 > Co–Mo/$MgAl_2O_4$ > Co–Mo/Al_2O_3). As expected, the CO conversion increases with the increase of the potassium loading. The optimum potassium loadings express as the amounts of K_2O, were 4%, 6%, and 6% on Co–Mo–K/MgO–Al_2O_3, Co–Mo–K/Al_2O_3, and Co–Mo–K/$MgAl_2O_4$ catalysts, respectively. In those cases, CO conversions for the reaction are closed to their equilibrium values.

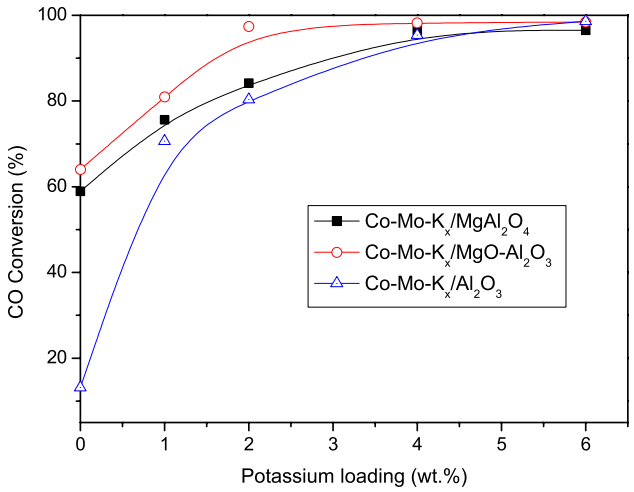

Fig. 2 Effect of potassium loading on the CO conversion over Co–Mo-based catalysts. *Reaction conditions*: 220 °C, total pressure = 2.0 MPa, GHSV = 2500 h^{-1}, and steam gas ratio = 0.6

Figure 3 shows the performances of the optimized potassium-doped and potassium-free catalysts as a function of reaction temperature. The activity of Co–Mo–K_6/Al_2O_3 catalyst decreased with the increase of temperature. However, the activities of Co–Mo–K_4/MgO–Al_2O_3 and Co–Mo/MgO–Al_2O_3 catalysts increased with the increase of temperature ranging from 200 to 400 °C then decreased slightly. Totally, the Co–Mo–K_6/Al_2O_3 catalyst manifests more distinct advantages than Co–Mo–K_4/MgO–Al_2O_3 catalyst or Co–Mo/MgO–Al_2O_3 catalyst at low temperature (200–270 °C). While the MgO–Al_2O_3 supported Co–Mo catalysts, with or without potassium additive, exhibit higher activities at high temperature (360–450 °C). Therefore, it is promising that Co–Mo–K/MgO–Al_2O_3 (or Co–Mo/MgO–Al_2O_3) catalysts and Co–Mo–K/Al_2O_3

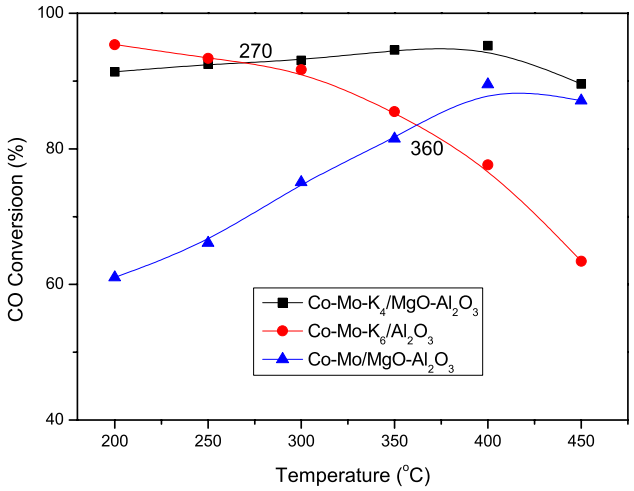

Fig. 3 Effect of temperature on the CO conversion over the Co–Mo-based catalysts. *Reaction conditions*: total pressure = 2.0 MPa, GHSV = 3000 h^{-1}, and steam gas ratio = 0.5

catalysts could be used in high-temperature shift stage and low-temperature shift stage, respectively. Since Co–Mo–K/MgO–Al_2O_3 (or Co–Mo/MgO–Al_2O_3) catalysts and Co–Mo–K/Al_2O_3 catalysts are sulfur-tolerant. Thus, they could be applied in coal- and heavy oil-derived feedstocks.

The deteriorative conditions were designed for testing the stability of the catalysts of Co–Mo–K_6/Al_2O_3, Co–Mo–K_4/MgO–Al_2O_3, and Co–Mo/MgO–Al_2O_3. The results are presented in Fig. 4. Under the conditions of temperature of 400 °C, total pressure of 2.0 MPa, GHSV of 15,000 h^{-1}, and steam gas ratio of 0.3, a steady loss of catalytic activity with the reaction time was observed over three catalysts. The rate of deactivation of Co–Mo–K_6/γ-Al_2O_3 catalyst is much quicker than that of MgO–Al_2O_3-supported catalysts (Co–Mo–K_4/MgO–Al_2O_3 and Co–Mo/MgO–Al_2O_3 catalysts). From 4 h on stream to 20 h, the decrease of the activity of Co–Mo/MgO–Al_2O_3 catalyst is negligible (decreased by ~3.7%), while the Co–Mo–K_6/γ-Al_2O_3 catalyst suffered a serious deactivation (decreased by ~30%). After 12 h on stream, the activity of Co–Mo–K_4/MgO–Al_2O_3 is almost the same as that of Co–Mo/MgO–Al_2O_3. This suggests that the loss of molybdenum and/or cobalt is not a key factor for the deactivation of Co–Mo–K catalysts. It is probably that the high dispersion of the Mo and Co components leads to a strong interaction between these components and support. As well-known, potassium ions are soluble and mobile and closely connected with the WGSR activity, therefore the potassium loss is responsible for the deactivation of K-containing catalysts. As shown in Fig. 4, the potassium-free Co–Mo/MgO–Al_2O_3 catalyst exhibited the highest stability.

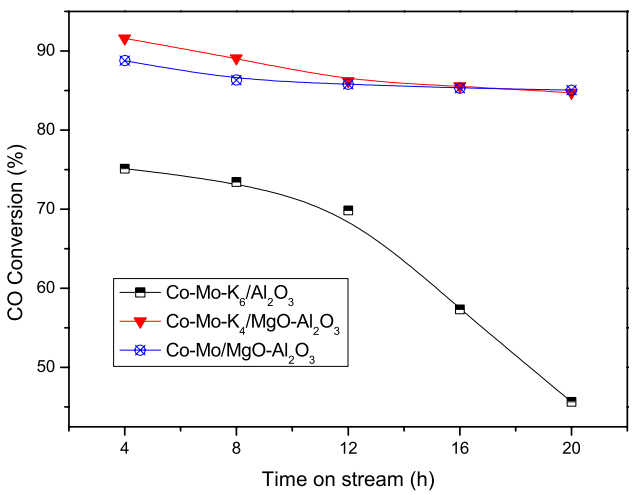

Fig. 4 Stability of Co–Mo-based catalysts as a function of reaction time. *Reaction conditions*: temperature = 400 °C, total pressure = 2.0 MPa, GHSV = 15,000 h^{-1}, and steam gas ratio = 0.3

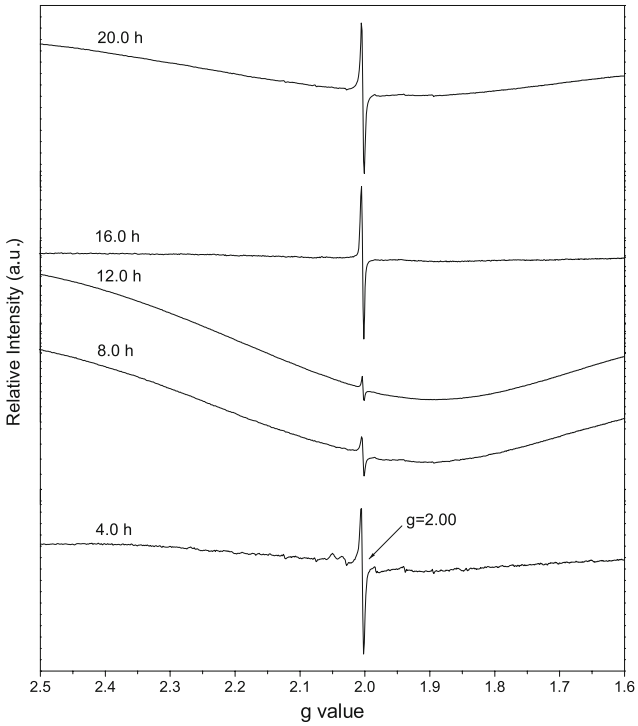

Fig. 5 ESR spectra of the tested Co–Mo–K_4/MgO–Al_2O_3 catalyst with different time on steam. Reaction conditions of the catalyst: temperature = 400 °C, total pressure = 2.0 MPa, GHSV = 15,000 h^{-1}, steam gas ratio = 0.3

3.3 ESR Characterization

Figure 5 shows the ESR spectra of the tested Co–Mo–K/MgO–Al_2O_3 catalysts with different time on steam. The signal of $g = 2.00$ is assigned to the oxysulfo-Mo^{5+} species [17, 30]. Interestingly, the oxo-Mo^{5+} species (g value is expected to be 1.93 [17]) were not observed in this study. It is probable that the MoO_3 species are monolayer-like dispersion on the support, making the terminal oxygen ligands easily contact with CS_2/H_2 in the pre-sulfidation. As shown in Fig. 5, the intensity of signal of $g = 2.0$ decreased with the increase of reaction time and reach a minimum value at 12 h. Thereafter, the intensity of oxysulfo-Mo^{5+} species increased with the increase of reaction time. It is probably that the potassium loss reaches a maximum value for the Co–Mo–K_4/MgO–Al_2O_3 catalyst and thereafter magnesium plays a leading role on Mo species.

4 Discussion

Two mechanisms have been proposed for the WGSR, i.e., an associative mechanism and a regenerative (or redox) mechanism [7]. The former mechanism suggests that the decomposition of the formate species intermediate forms

CO_2 and H_2, while the latter mechanism suggests that the formation of H_2 proceeds via a reduction process (H_2O + Red → H_2 + Ox) and CO_2 via an oxidation process (CO + Ox → CO_2 + Red). Hou et al. [8] proposed that the WGSR mechanism involves a Mo^{5+}/Mo^{4+} redox cycle on the sulfided Mo/Al_2O_3 catalysts (Scheme 1).

To verify the importance of Mo^{5+} species, the ESR measurements were carried out for the tested catalyst (Fig. 5). With the gradual deactivation of the Co–Mo–K/$MgO–Al_2O_3$ as a function of reaction time, the intensity of oxysulfo-Mo^{5+} should have decreased linearly with the increase of the reaction time. However, the results of ESR characterization in this study suggest that the Mo^{5+} species are not related to the WGS activity. This indicates that the regenerative mechanism may not be operative on the alkali-doped Co–Mo catalysts. Łaniecki and Zmierczak [13] observed the similar results over the Y-zeolite-supported Mo-based catalysts. In their case, the catalysts prepared from hexacarbonyl molybdenum are more active than those from ammonium heptamolybdate; however, the signal of Mo^{5+} species appeared only on the samples prepared from ammonium heptamolybdate. The base-doped Mo-based and Cu-based catalysts were suggested to be the bifunctional catalysts and therein the function of alkali metals was suggested to favor the reaction of CO with oxygen anions to produce formate species [19, 31]. Very recently, Rodriguez et al. [4] studied the WGSR on the $Au–TiO_2$ and $Au–CeO_2$ catalysts. They pointed out that H_2O dissociates on oxides to form OH_{ads}, with which the adsorbed CO on Au reacts to produce $HOCO_{ads}$, and the subsequent decomposition of the surface formate species forms CO_2 and H_{ads}. In this study, since the alkali components themselves do not provide sites for CO adsorption, the Co–Mo species thus may be analogy to the Au species in [4]. With the addition of magnesium as a base to Al_2O_3, the Co–Mo/$MgO–Al_2O_3$ catalysts became the acid–base catalysts. The basic components could induce the counterion, i.e., formate species, which are proposed as the intermediate for the WGSR [7, 19, 32]. Therefore, it is observed that the activities of samples, expressed by CO

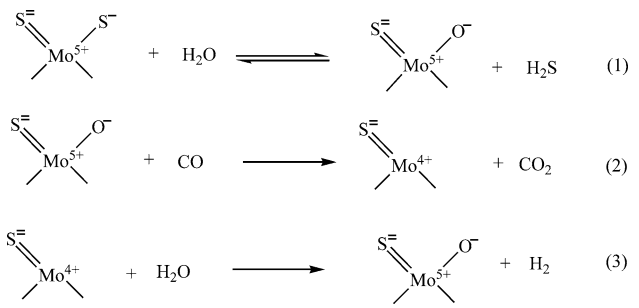

Scheme 1 Proposed WGSR mechanism over sulfided Mo/Al_2O_3 catalysts [8]

conversion, decrease in the following order: Co–Mo–K/$MgO–Al_2O_3$ > Co–Mo/$MgO–Al_2O_3$ > Co–Mo/Al_2O_3 (as shown in Fig. 2). Evin et al. [33] further proposed that appropriate amounts of alkali doping on Pt/Ceria catalysts facilitate formate C–H bond cleaving, which promotes the WGSR.

The structure of $MgAl_2O_4$ spinel is similar to that of γ-Al_2O_3, while the difference lies in the numbers of cations distributed among the oxygen ions [34]. The introduction of Mg^{2+} inhibits alumina sintering but maintains its pore structure. Moreover, the addition of magnesia neutralizes the acidity of alumina [27]. Morterra et al. [35] reported that the new Lewis acid sites (Mg^{2+}) are formed on the surface of $MgAl_2O_4$ spinel. Compared to the $MgO–Al_2O_3$ mixed oxides support, as predicted, most of Mg^{2+} are infiltrated into the crystal lattice of the $MgAl_2O_4$ spinel support. This can explain the facts that the WGS activities are in the order of Co–Mo/$MgO–Al_2O_3$ > Co–Mo/$MgAl_2O_4$ > Co–Mo/Al_2O_3 in our present conditions (as shown in Fig. 2). Accordingly, the $MgO–Al_2O_3$ mixed oxides could serve as an excellent support for the Co–Mo-based sulfur-tolerant water–gas shift catalysts. Usually, the operating temperature window of Co–Mo-based catalysts is 250–500 °C. At higher temperatures, the metal sulfides are more easily transformed into metal oxides (e.g., Reaction (1) shown in Scheme 1). Thus, the feedstock should be containing sufficient sulfur to maintain a viable activity [36]. This effect can explain that the activities of Co–Mo–K_4/$MgO–Al_2O_3$ and Co–Mo/$MgO–Al_2O_3$ catalysts reach to a maximum at 400 °C and then decrease slightly (as shown in Fig. 3).

Whatever the supports are used for the Co–Mo–K catalysts, the potassium loss takes place inevitably (Fig. 4). The potassium-free catalyst, i.e., Co–Mo/$MgO–Al_2O_3$, shows higher stability for the WGSR. It can be explained that the surface Mg^{2+} and/or MgO species anchoring in the supports serves as basic components (Fig. 1), which are less motional than potassium. The basicity of Mg^{2+} is weaker than that of K^+. The potassium additive favors the formation of K^+–$HOCO_{ads}$, but its weaker nucleophilic character makes the formate species less stable, while the magnesium additive does not favor the formation of Mg^{2+}–$HOCO_{ads}$, but its stronger nucleophilic character makes the formate species more stable. Thus, the activities of Co–Mo/$MgO–Al_2O_3$ catalysts are higher than those of Co–Mo–K/Al_2O_3 catalysts at high temperature (360–450 °C), and the Co–Mo–K/Al_2O_3 catalysts are more suitable for low-temperature shift (200–270 °C) (Fig. 3). Since WGSR is a reversible, exothermic reaction ($\Delta H = -41.1$ kJ mol^{-1}), the WGS process involves multiple or two stages using Fe–Cr or Cu–Zn catalysts that fit for each stage [7]. Likewise, Co–Mo/$MgO–Al_2O_3$ and Co–Mo–K/Al_2O_3 catalysts could be fitted the different stages as the sulfur-tolerant WGSR catalysts.

5 Conclusions

In this work, the $MgO–Al_2O_3$ mixed oxides were prepared and used as the support of Co–Mo-based WGSR catalysts. The $MgO–Al_2O_3$-supported Co–Mo-based catalysts exhibit higher activities than those of $MgAl_2O_4$-supported Co–Mo-based catalysts. The addition of potassium enhances the activities, but affects adversely the stabilities of Co–Mo-based catalysts. The $Co–Mo/MgO–Al_2O_3$ catalysts could be used as the high-temperature shift catalysts. XRD characterization shows the $MgO–Al_2O_3$ support is composed of mixed oxides of MgO, γ-Al_2O_3, and $MgAl_2O_4$. ESR characterization shows that the Mo^{5+} species are not connected with the WGSR activity. Magnesium in the support may be closely related with the formation of formate species intermediate for the WGSR.

Acknowledgments This work was supported by Fujian Province Science and Technology Project and Xiamen Municipal Science and Technology Project.

References

1. Newsome DS (1980) Catal Rev Sci Eng 21:275
2. Hutchings GJ, Copperthwaitet RG, Gottschalk FM, Hunter R, Mellor J, Walter Orchard S, Sangiorgio T (1992) J Catal 137:408
3. Rhodes C, Hutchings GJ (2003) Phys Chem Chem Phys 5:2719
4. Rodriguez JA, Ma S, Liu P, Hrbek J, Evans J, Pérez M (2007) Science 318:1757
5. Pierre D, Deng W, Flytzai-Stephanopoulos M (2007) Top Catal 46:363
6. Azzam KG, Babich IV, Seshan K, Lefferts L (2008) Appl Catal B 80:129
7. Rhodes C, Hutchings GJ, Ward AM (1995) Catal Today 23:43
8. Hou P, Meeker D, Wise H (1983) J Catal 80:280
9. Kantschewa M, Delannay F, Jeziorowski H, Delgado E, Eder S, Ertl G, Knözinger H (1984) J Catal 87:482
10. Kettmann V, Balgavý P, Sokol L (1988) J Catal 112:93
11. Xie X, Yin H, Dou B, Hou J (1991) Appl Catal 77:187
12. Hakkarainena R, Salmi T, Keiskib RL (1993) Appl Catal A 99:195
13. Łaniecki M, Zmierczak W (1991) Zeolites 11:18
14. Lund CRF (1996) Ind Eng Chem Res 35:2531
15. Nickolov RN, Edreva-Kardjieva RM, Kafedjiysky VJ, Nikolova DA, Stankova NB, Mehandjiev DR (2000) Appl Catal 190:191
16. Łaniecki M, Małecka-Grycz M, Domka F (2000) Appl Catal A 196:293
17. Nikolova D, Edreva-Kardjieva R, Gouliev G, Grozeva T, Tzvetkov P (2006) Appl Catal A 297:135
18. Łaniecki M, Ignacik M (2006) Catal Today 116:400
19. Klier K (1992) Catal Today 15:361
20. Shen J (2001) Synthesis of ammonia. Chemical Industry Press, Beijing, China
21. Mross WD (1983) Catal Rev Sci Eng 25:591
22. Lorenz E, Wodtck F, Ebenhoech FL, Giesler E (1970) US patent 3 529 935
23. Merriam JS, Hogg CB (1984) US patent 4 452 854
24. Patt J, Moon DJ, Phillips C, Thompson L (2000) Catal Lett 65:193
25. Nagai M, Matsuda K (2006) J Catal 238:489
26. Wen W, Calderon JE, Brito JL, Marinkovic N, Hanson JC, Rodriguez JA (2008) J Phys Chem C 112:2121
27. Houssenbay S, Payen E, Kasztelan S, Grimblot J (1991) Catal Today 10:541
28. Vrieland GE, Khazai B, Murchison CB (1996) Appl Catal A 134:1123
29. Zhang Y, Dou B, Xie X (1992) React Kinet Catal Lett 48:135
30. Weber Th, Muijsers JC, van Wolput JHMC, Niemantsverdriet JW (1996) J Phys Chem 100:14144
31. Gotti A, Prins R (1998) J Catal 178:511
32. Amenomiya Y, Pleizier G (1982) J Catal 76:345
33. Evin HN, Jacobs G, Thomas GA, Davis BH (2008) Catal Lett 120:166
34. Jiang R, Xie Z, Zhang C, Chen Q (2004) Catal Today 359:93–95
35. Morterra C, Ghiotti G, Boccuzi F, Coluccia S (1978) J Catal 51:299
36. de Bruijn FA, Rietveld B, van den Brink RW (2007) In: Centi G, van Santen Rutger A (eds) Catalysis for renewables: from feedstock to energy production. Wiley-VCH, Weinheim, Germany